Microfluidics

Deutsche Ausgabe: DOI: 10.1002/ange.201502886
Internationale Ausgabe: DOI: 10.1002/anie.201502886

Microfluidic Formation of Membrane-Free Aqueous Coacervate Droplets in Water**

Dirk van Swaay, T.-Y. Dora Tang, Stephen Mann, and Andrew de Mello**

Abstract: *We report on the formation of coacervate droplets from poly(diallyldimethylammonium chloride) with either adenosine triphosphate or carboxymethyl-dextran using a microfluidic flow-focusing system. The formed droplets exhibit improved stability and narrower size distributions for both coacervate compositions when compared to the conventional vortex dispersion techniques. We also demonstrate the use of two parallel flow-focusing channels for the simultaneous formation and co-location of two distinct populations of coacervate droplets containing different DNA oligonucleotides, and that the populations can coexist in close proximity up to 48 h without detectable exchange of genetic information. Our results show that the observed improvements in droplet stability and size distribution may be scaled with ease. In addition, the ability to encapsulate different materials into coacervate droplets using a microfluidic channel structure allows for their use as cell-mimicking compartments.*

Protocells are synthetic microsystems that mimic many basic properties of natural cells such as compartmentalization, metabolism, and replication and are of significant interest in research on living technologies, synthetic biology, and the origin of life.[1,2] Of these, compartmentalization is a key property that has been increasingly studied due to its potential application in bioreactors, drug delivery mechanisms, and artificial cellular platforms.[3–6] In recent years, a range of microfluidic technologies have been shown to be advantageous in realizing chemical and biological compartmentalization, and in addition are accompanied by significant improvements in analytical performance, experimental control, and increased experimental throughput.[7–10] Of particular interest has been the encapsulation of chemical or biological materials in sub-nanoliter aqueous droplets contained within fluorinated oils.[11–15] To date, the function of the continuous phase in water-in-oil droplet systems has typically been restricted to the simple separation and isolation of the material of interest. In contrast, the external medium is fundamentally important in a biological context, in which compartmentalization can be achieved by means of a semi-permeable lipid membrane that separates intra- and extracellular aqueous environments.[16–18] However, compartmentalization that exhibits properties of selective permeability and encapsulation of biological components may also be realized without the need for a membrane. Membrane-free coacervate droplets, formed by aqueous–aqueous phase separation offer an alternative model for synthetic cells.[19,20] Droplet formation is driven by electrostatic and entropic interactions between dilute solutions of charged polymers or macromolecules and results in the formation of component-enriched microdroplets suspended in a chemically depleted aqueous continuous phase.[21] Coacervate microdroplets have been shown to form between a diverse range of charged molecules such as biological macromolecules, synthetic and natural polymers, as well as low molecular weight components such as cationic oligolysine and nucleotides such as adenosine triphosphate (ATP).[20–24] Importantly, the molecularly crowded environment inside a coacervate droplet is akin to that encountered within natural cells, providing a useful and relevant artificial cell model.[20,25] In addition, coacervate microcompartments have been shown to exhibit selective molecular sequestration due to a lower dielectric constant than the continuous water phase and to encapsulate enzymatic reactions displaying enhanced catalytic activity.[26,27] These properties make coacervate droplets promising bioreactors. However, coacervate microdroplets formed by conventional methods are limited in their application as artificial cellular platforms due to their polydispersity and instability to coalescence. In the present study, we address these shortcomings by exploiting microfluidic technology to rapidly and controllably form large populations of coacervate microdroplets of narrow size distribution, capable of encapsulating DNA molecules, and which exhibit increased stability in water without the need for any surfactants or other stabilizing agents.

Coacervate microdroplets were formed by dispersion of a bulk coacervate phase—either poly(diallyldimethylammonium chloride) (PDDA) and ATP (4:1 molar ratio) or PDDA and carboxymethyl-dextran (CM-dextran) (1:3 molar ratio) at pH 8 (See the Experimental Section)—into deionized water. As the PDDA/ATP and PDDA/CM-dextran coacervate mixtures were composed primarily of long-chain polyelectrolyte molecules, the resulting fluids were viscoelastic or non-Newtonian in nature with extremely low surface interfacial tension (42 ± 0.2 mN m^{-1} for 4:1 PDDA/ATP coacervate).[21] Both these properties have important implications for the

[*] D. van Swaay,[+] Prof. Dr. A. de Mello
Institute for Chemical and Bioengineering, ETH Zurich
Wolfgang-Pauli-Str. 10, 8093 Zurich (Switzerland)
E-mail: andrew.demello@chem.ethz.ch
Dr. T.-Y. D. Tang,[+] Prof. Dr. S. Mann
Centre for Protolife Research, Centre for Organized Matter
School of Chemistry, University of Bristol
Bristol, BS8 1TS (UK)
E-mail: s.mann@bristol.ac.uk
[+] These authors contributed equally to this work.

[**] We thank the Engineering and Physical Sciences Research Council (EPSRC (UK)), the European Research Council (Advanced Grant), and ETH Zürich for financial support.
Supporting information for this article is available on the WWW under http://dx.doi.org/10.1002/anie.201502886.

break-up mechanism of the bulk coacervate fluid into droplets within a microfluidic environment. Contrary to simple immiscible fluid droplet systems that rely on surface tension and Plateau–Rayleigh instabilities for breaking-up a continuous stream into droplets,[28–30] break-up of the coacervate stream within a laminar flow configuration requires the continuous shearing of material into a filament until it is able to segment. For this, we employed a microfluidic flow-focusing channel structure to disperse a continuous aqueous coacervate stream into membrane-free coacervate droplets in water (Figure 1a). The microfluidic device was

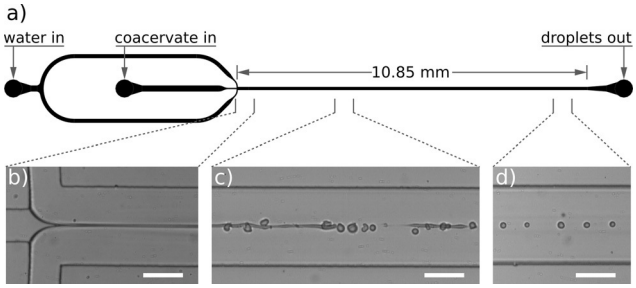

Figure 1. a) Schematic of the microfluidic flow-focusing channel structure used to disperse bulk coacervates into water. All channels are 40 μm in height. The main channel is 10.85 mm long and 100 μm wide, whereas the three channels entering the junction are 40 μm wide. b) The bulk coacervate phase enters the junction from the channel to the left, and is pinched and focused by a much faster sheath flow of water entering the junction from the channels at the top and bottom. The focused jet of coacervate flows along the channel to the right, in which c) it breaks into segments and d) recoils into spherical droplets. Scale bars are 50 μm. The exact location of the break-up along the channel varies, depending on pressure and coacervate viscosity.

prepared by conventional soft lithography techniques using polydimethylsiloxane (PDMS) silicone elastomer[31] and treated with 5% 1*H*,1*H*,2*H*,2*H*-perfluorooctyltrichlorosilane (PFOS) to minimize interactions between the coacervate fluid and PDMS channel surfaces (see the Supporting Information). Video images of the break-up mechanism show that the focused jet of coacervate fluid initially forms a continuous viscoelastic stream confined between the flowing water channels. This is followed by segmentation of the coacervate filament and reorganization of the isolated linear fragments into spherical droplets (Figure 1b–d and Video S1). Interestingly, break-up of the coacervate stream required considerably more time and occurred over much longer lengths (millimeters rather than microns) than typically observed for the segmentation of immiscible phases.[32–34] These observations are consistent with alignment of the polymer molecules parallel to the filament prior to segmentation within the laminar flow, and a polymer recoil mechanism for formation of the droplets during the collapse of the stretched coacervate filament.[35] Significantly, when formed in this manner, the membrane-free polymer/nucleotide or polymer/polysaccharide coacervate droplets did not merge readily when coming into contact, even over prolonged periods of time (Figures 2a and S1a). Long-term incubation

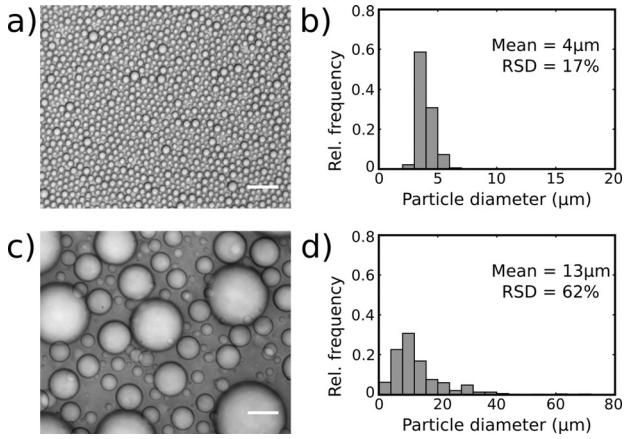

Figure 2. A comparison of the size distribution of PDDA/ATP coacervate droplets formed a) in the microfluidic device shown in Figure 1 and c) using the vortex method, with respective histograms (b and d) showing the size distribution for each population. All scale bars are 25 μm.

studies demonstrated that populations of closely packed droplets in water persisted with little or no coalescence for more than six days at room temperature (Figure S2). This is in stark contrast to PDDA/ATP (Figure 2c) or PDDA/CM-dextran coacervate droplets (Figure S1b) formed under turbulent flow conditions (i.e., formed by vortex-induced mixing of a bulk coacervate liquid and water), which readily coalesced over seconds (Figure S1b). Figure S3 shows the equivalent data for the formation of PDDA/CM-dextran coacervate microdroplets. Size analysis of droplets (see Supporting Information), collected into 96-well plates, indicated that dispersion of the coacervate using a microfluidic flow-focusing geometry results in a significantly narrower droplet size distribution when compared to populations produced using the vortex method (Figure 2a–d, Table S1). PDDA/ATP droplets obtained by microfluidic flow-focusing were on average 4 μm in diameter with a relative standard deviation (RSD) of 17%; by comparison, PDDA/ATP droplets formed by the vortex method had a mean diameter of 13 μm and a RSD of 62%. Likewise, droplets from the PDDA/CM-dextran coacervate population had a mean diameter of 8 μm with a RSD of 17% when prepared by the microfluidic method, and a mean diameter of 6 μm with a 45% RSD when prepared by vortexing.

We then used a device containing two parallel flow-focusing geometries that converge close to the exit to prepare two distinct populations of polymer/nucleotide or polymer/polysaccharide coacervate droplets simultaneously which then mixed whilst exiting the device. Moreover, to test whether genetic information could be immobilized within or transferred between adjacent droplets, single-stranded (ss) DNA oligonucleotides labeled with either fluorescein or cyanine 5 (Cy5) (on the 3′ or 5′ ends, respectively) were added to the continuous coacervate streams (Figure 3a). The mixed droplets were then loaded into 96-well plates for storage, imaging, and analysis. Following collection, fluorescence images of the ssDNA-containing PDDA/ATP (Figure 3b–e) or PDDA/CM-dextran (Figure S4) coacervate droplets were

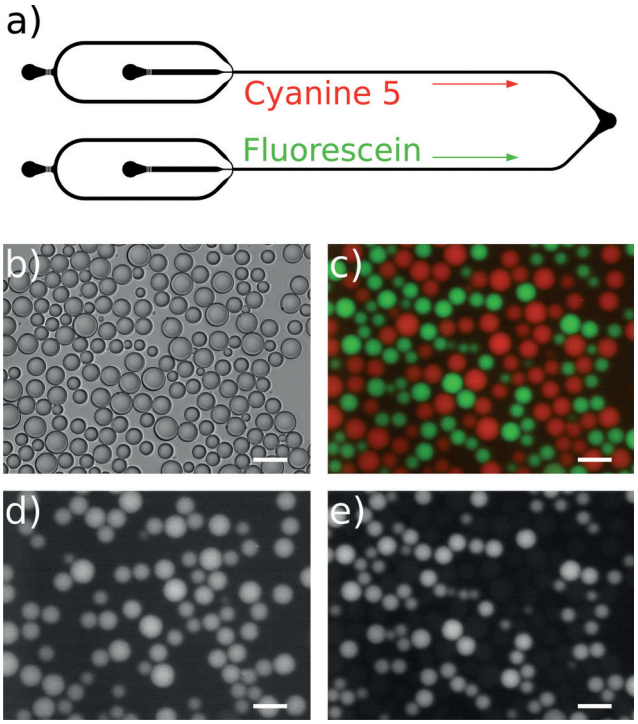

Figure 3. a) A schematic diagram of the parallel flow-focusing microfluidic channel structure. Bulk coacervate containing Cyanine 5 and fluorescein-labeled ssDNA oligonucleotides are simultaneously focused into streams of water in the top and bottom channels respectively. The two parallel streams then converge at the outlet on the right hand side. b) A bright-field micrograph of PDDA/ATP coacervate droplets containing the different labels collected from the parallel device. c) A composite image of both Cyanine 5 (red) and fluorescein (green) fluorescence imaging channels showing the two separate populations of ssDNA-containing droplets coexisting without merging. d) and e) show the single channel images for Cyanine 5 and fluorescein, respectively. All scale bars are 25 μm.

measured using filter sets for both dyes (see the Experimental Section). Analysis of the populations of droplets indicated that droplets from both populations remain distinct with little to no change in the number of droplets exhibiting both Cy5 or fluorescein between $t = 0$ and $t = 48$ h (Table S2). Control experiments performed with coacervate droplets containing a mixture of both dyes showed fluorescence signals from both Cy5- and fluorescein-labeled DNA oligonucleotides (Figure S5), indicating that any significant exchange of the genetic polymers between distinct populations would be detectable using the filter sets employed.

In summary, we have shown that membrane-free aqueous polymer/nucleotide or polymer/polysaccharide coacervate droplets can be formed in water using a microfluidic flow-focusing channel structure, and that this technique offers unique advantages compared to traditional vortexing methods. The excellent stability of the droplet suspensions at room temperature and for periods longer than six days was achieved through the laminar flow break-up process afforded by the low Reynolds number ($Re < 2100$) regime encountered in the microfluidic system. The approach also offers the ability to form distinct coacervate populations of differing chemical composition in parallel, without detriment to coacervate stability or size distribution. Droplets formed using two parallel flow-focusing channels also exhibit a narrower size distribution (Figure S6)—albeit with a small variation in mean droplet diameter between channels due to small differences in flow rates—and improved droplet stability when compared to those formed using the vortex method, confirming that the advantages conferred by the single-channel device are preserved when the process is scaled. The ability to simultaneously produce distinct droplet populations with similar characteristics is an additional and unique capability of the microfluidic method that cannot be reproduced using other techniques, and which opens up opportunities to perform studies involving transport as well as chemical and biological interactions between droplets loaded with different materials. In particular, we have demonstrated that it is possible to prepare and co-locate simultaneously two populations of coacervate droplets containing different DNA oligonucleotides, and that the populations can coexist in close proximity for up to 48 h without detectable exchange of genetic information. These observations suggest that our method may be adapted for the study of directed evolution processes in membrane-free coacervate droplets,[36,37] and thus provides a significant step toward studying interactions between coacervate droplets hosting diverse functional materials. In this regard, we are currently investigating the encapsulation of cellular components such as machinery for gene expression and protein synthesis to test the viability of coacervate droplets as artificial protocellular systems.

Experimental Section

Coacervate preparation and dispersion. Bulk coacervate phase was prepared for dispersion within the microfluidic device by adopting the following procedure. Coacervate droplets were prepared by mixing equimolar solutions (100 mM) of 8.5 kDa poly(diallyldimethylammonium chloride) (PDDA) with either carboxymethyl-dextran or adenosine triphosphate (ATP) prepared at pH 8 to obtain a final total PDDA monomer:ATP molar ratio of 4:1 or a total PDDA monomer:CM-dextran monomer ratio of 1:3. The coacervate phase was then separated by centrifugation of the dispersion for at least 20 min at 5000 rpm and isolated by removing the supernatant. For fluorescence experiments, dye-labeled oligonucleotides GTTAGCAGCCGGATCTCAGTGGT with fluorescein on 3′ end, MW = 7662 g mol^{-1}, and ACCACTGAGATCCGGCTGCTAAC with Cy5 on 5′ end, MW = 7635 g mol^{-1}, Eurofins Genomics, Germany) were mixed into different coacervate dispersions prior to centrifugation and isolation. For control experiments the two dye-labeled oligos were premixed and then added to the coacervate dispersion prior to bulk phase preparation. In all instances the initial oligonucleotide stock solution (16.7 μM) was diluted 2500 times (PDDA/ATP) or 6000 times (CM-dextran/PDDA). Bulk coacervate (with and without oligonucleotides) was dispersed in DI water within the microfluidic device using Dolomite pressure pumps.

Fluorescence imaging. Fluorescence images of ssDNA-containing droplets were measured using appropriate filter sets for each dye (for fluorescein, 475/28 nm excitation and 560/40 nm emission, 518 nm dichroic mirror; for Cy5, 626/40 nm excitation and 655 nm long-pass emission, 648 nm dichroic mirror). Imaging was performed using an inverted microscope (Eclipse Ti-U, Nikon, Japan) with a wide-field camera (CoolSNAP HQ2, Photometrics, USA). Exposure and acquisition was controlled using Micro Manager software.[38]

Keywords: coacervate · microfluidics · microreactors · polymers · protocells

How to cite: *Angew. Chem. Int. Ed.* **2015**, *54*, 8398–8401
Angew. Chem. **2015**, *127*, 8518–8521

[1] P. Walde, *Bioessays* **2010**, *32*, 296–303.
[2] A. J. Dzieciol, S. Mann, *Chem. Soc. Rev.* **2012**, *41*, 79–85.
[3] P.-A. Monnard, H.-J. Ziock, *Origins Life Evol. Biospheres* **2007**, *37*, 469–472.
[4] V. Noireaux, A. Libchaber, *Proc. Natl. Acad. Sci. USA* **2004**, *101*, 17669–17674.
[5] A. Pohorille, D. Deamer, *Trends Biotechnol.* **2002**, *20*, 123–128.
[6] P. Stano, P. L. Luisi, *Chem. Commun.* **2010**, *46*, 3639.
[7] B. M. Paegel, *Curr. Opin. Chem. Biol.* **2010**, *14*, 568–573.
[8] S. Matosevic, B. M. Paegel, *J. Am. Chem. Soc.* **2011**, *133*, 2798–2800.
[9] M. Karlsson, M. Davidson, R. Karlsson, A. Karlsson, J. Bergenholtz, Z. Konkoli, A. Jesorka, T. Lobovkina, J. Hurtig, M. Voinova, et al., *Annu. Rev. Phys. Chem.* **2004**, *55*, 613–649.
[10] P. S. Dittrich, M. Jahnz, P. Schwille, *ChemBioChem* **2005**, *6*, 811–814.
[11] X. i Solvas, A. deMello, *Chem. Commun.* **2011**, *47*, 1936–1942.
[12] A. Huebner, S. Sharma, M. Srisa-Art, F. Hollfelder, J. B. Edel, A. J. deMello, *Lab Chip* **2008**, *8*, 1244–1254.
[13] L. Mazutis, J.-C. Baret, P. Treacy, Y. Skhiri, A. F. Araghi, M. Ryckelynck, V. Taly, A. D. Griffiths, *Lab Chip* **2009**, DOI: 10.1039/b907753g.
[14] E. Sokolova, E. Spruijt, M. M. K. Hansen, E. Dubuc, J. Groen, V. Chokkalingam, A. Piruska, H. A. Heus, W. T. S. Huck, *Proc. Natl. Acad. Sci. USA* **2013**, *110*, 11692–11697.
[15] S.-Y. Teh, R. Lin, L.-H. Hung, A. P. Lee, *Lab Chip* **2008**, *8*, 198–220.
[16] B. Alberts, A. Johnson, J. Lewis, D. Morgan, M. Raff, K. Roberts, P. Walter, *Molecular Biology of the Cell*, Garland Science **2014**.
[17] D. A. Brafman, S. de Minicis, E. Seki, K. D. Shah, D. Teng, D. Brenner, K. Willert, S. Chien, *Integr. Biol.* **2009**, *1*, 513–524.
[18] G. Charras, E. Sahai, *Nat. Rev. Mol. Cell Biol.* **2014**, *15*, 813–824.
[19] H. G. Bungenberg de Jong, *Protoplasma* **1932**, *15*, 110–173.
[20] S. Koga, D. S. Williams, A. W. Perriman, S. Mann, *Nat. Chem.* **2011**, *3*, 720–724.
[21] D. S. Williams, S. Koga, C. R. C. Hak, A. Majrekar, A. J. Patil, A. W. Perriman, S. Mann, *Soft Matter* **2012**, *8*, 6004–6014.
[22] C. G. de Kruif, F. Weinbreck, R. de Vries, *Curr. Opin. Colloid Interface Sci.* **2004**, *9*, 340–349.
[23] D. Priftis, K. Megley, N. Laugel, M. Tirrell, *J. Colloid Interface Sci.* **2013**, *398*, 39–50.
[24] D. Priftis, N. Laugel, M. Tirrell, *Langmuir* **2012**, *28*, 15947–15957.
[25] S. Mann, *Acc. Chem. Res.* **2012**, *45*, 2131–2141.
[26] T.-Y. D. Tang, M. Antognozzi, J. A. Vicary, A. W. Perriman, S. Mann, *Soft Matter* **2013**, *9*, 7647–7656.
[27] J. Crosby, T. Treadwell, M. Hammerton, K. Vasilakis, M. P. Crump, D. S. Williams, S. Mann, *Chem. Commun.* **2012**, *48*, 11832–11834.
[28] J. Plateau, *Expérimentale et Théorique Des Liquides Soumis Aux Seules Forces Moléculaires*, Gauthier-Villars, Paris, **1873**.
[29] Lord Rayleigh, *Philos. Mag. Ser. 5* **1892**, *34*, 145–154.
[30] J. Eggers, *Rev. Mod. Phys.* **1997**, *69*, 865–930.
[31] Y. Xia, G. M. Whitesides, *Angew. Chem. Int. Ed.* **1998**, *37*, 550–575; *Angew. Chem.* **1998**, *110*, 568–594.
[32] R. Sattler, S. Gier, J. Eggers, C. Wagner, *Phys. Fluids* **2012**, *24*, 023101.
[33] J. Tan, J. H. Xu, S. W. Li, G. S. Luo, *Chem. Eng. J.* **2008**, *136*, 306–311.
[34] Q. Xu, M. Nakajima, *Appl. Phys. Lett.* **2004**, *85*, 3726–3728.
[35] D. T. Papageorgiou, *Phys. Fluids* **1995**, *7*, 1529–1544.
[36] A. Fallah-Araghi, J.-C. Baret, M. Ryckelynck, A. D. Griffiths, *Lab Chip* **2012**, *12*, 882–891.
[37] J. J. Agresti, E. Antipov, A. R. Abate, K. Ahn, A. C. Rowat, J.-C. Baret, M. Marquez, A. M. Klibanov, A. D. Griffiths, D. A. Weitz, *Proc. Natl. Acad. Sci. USA* **2010**, *107*, 4004–4009.
[38] A. Edelstein, N. Amodaj, K. Hoover, R. Vale, N. Stuurman, *Current Protocols Molecular Biology*, Wiley, New York, **2001**.

Received: March 29, 2015
Published online: May 27, 2015

